Study of the Characterization and Curing of a Phenyl Benzoxazine Using ^{15}N Solid-State Nuclear Magnetic Resonance Spectroscopy

VERNON M. RUSSELL, JACK L. KOENIG, HONG YEE LOW, HATSUO ISHIDA

Department of Macromolecular Science, Case Western Reserve University, Cleveland, Ohio 44106

Received 2 September 1997; accepted 16 November 1997

ABSTRACT: A difunctional 1,3-benzoxazine compound, 2,2′-(3-phenyl-4-dihydro-1,3,2-benzoxazine)propane (**B-a**), derived from bisphenol-A, ^{15}N-enriched aniline, and formaldehyde was synthesized and characterized using ^{15}N-NMR and ^{13}C-NMR spectroscopies. The observed resonances in the solid-state ^{15}N- and ^{13}C-NMR spectra showed good agreement with the calculated chemical shifts which are based on the chemical structure. The **B-a** samples were cured at 150 and 200°C. The polymerization inspired peak intensity changes and line-width broadenings in the NMR spectra. © 1998 John Wiley & Sons, Inc. J Appl Polym Sci 70: 1401–1411, 1998

Key words: benzoxazine; NMR; curing; characterization

INTRODUCTION

Difunctional benzoxazines are a relatively new type of phenolic resin. An extensive overview of phenolic resins and benzoxazines was conducted previously.[1] However, very little work has been done in the area of ^{15}N-NMR spectroscopy of these materials. The purpose of this work was to characterize 2,2′-(3-phenyl-4-dihydro-1,3,2-benzoxazine)propane (**B-a**) as well as to analyze the curing of this benzoxazine at two different cure temperatures using solid-state ^{15}N-NMR spectroscopy.

Solid-state NMR

Solid-state NMR has been used to study phenolic resins[2,3] as well as benzoxazines.[1,4] Further, there have been substantial ^{13}C chemical-shift assignments observed for benzoxazines.[5–7] However, there have been very few investigations of solid-state ^{15}N-NMR spectroscopy on these compounds.[8]

^{15}N Solid-state NMR Spectroscopy

The first reported nuclear magnetic resonance experiments utilizing the nitrogen isotopes (^{14}N and ^{15}N) took place in 1950.[9] The problems associated with the NMR of these nuclei include the fact that the ^{14}N nucleus has a spin quantum number of 1, which is associated with a quadrupolar moment. This results in a very efficient relaxation mechanism, making the spin–spin relaxation times very short. Because of this, the observed line widths in ^{14}N-NMR are very broad. The limitations for ^{15}N-NMR stem from the low natural abundance and low sensitivity of this isotope. This limitation can be overcome by isotopic enrichment, but this process is expensive and not always a straightforward procedure. The advent of the Fourier transform (FT) NMR technique greatly increased the feasibility of studies using nuclei of low sensitivity (^{13}C, ^{15}N) of natural abundance samples. In 1982, the first practical studies involving ^{15}N solid-state NMR of natural abundance samples

Correspondence to: J. L. Koenig.

Journal of Applied Polymer Science, Vol. 70, 1401–1411 (1998)
 CCC 0021-8995/98/071401-11

were reported[10,11] and utilized the general solid-state NMR techniques (cross polarization, high power proton decoupling, and magic angle spinning).

The major advantage of ^{15}N-NMR is its large range of chemical shifts compared to that of other nuclei. This range is approximately 1000 ppm. However, the practical chemical-shift range, especially for polymeric studies, is about 400 ppm. This is because polymer structures rarely contain nitroso groups and azo bridges which are found shifted far downfield. Further, there are fewer chemically distinct nitrogen groups compared to those of carbon, which results in simpler spectra. This makes spectral identification and quantitative analysis more straightforward.

Andreis and Koenig conducted a systematic review of the applications of ^{15}N-NMR to polymeric systems including substantial chemical-shift assignments.[12] Other overviews of ^{15}N-NMR spectroscopy have been made[13,14] and include references on coupling constants and group chemical-shift ranges.

Benzoxazine Curing

The polymer structure of the benzoxazine used in this research is significantly different from that of the monomer, that is, the breaking of the benzoxazine ring upon curing results in the formation of a nitrogen bridge structure. Since the environment of the nitrogens in this compound changes significantly, from a ring compound to a bridge structure, it should be possible to observe changes in the ^{15}N-NMR spectrum as polymerization proceeds.

EXPERIMENTAL

A 50/50 mixture of ^{15}N-enriched (98%) and natural abundance aniline was used to synthesize **B-a** using a procedure originally described by Ning and Ishida.[15] The synthesis reaction of **B-a** is shown in Figure 1. A portion of a polymer molecule of **B-a** is shown in Figure 2(a) along with potential crosslinks. The expected chemical shifts of both the monomer and polymer were calculated using reference compounds and correlations between ^{15}N and ^{13}C chemical shifts[16] and are given in Table I. All NMR experiments were performed on a Bruker MSL-300 spectrometer at a ^{15}N spectral frequency of 30.41 MHz. ^{15}N spectra were calibrated using ^{15}N-enriched glycine and set to the δ (NH_3) = 0 chemical-shift scale. Figure 3 shows some of the NMR pulse sequences used in this study. The acquisition techniques of cross polarization (CP), magic angle spinning (MAS), and high-power proton decoupling (DD) were used in this study. Variable contact time cross-polarization experiments were conducted to determine the optimum contact time. This contact time (3 ms) was used for all subsequent experiments utilizing cross polarization. The CP–MAS–DD spectrum of **B-a** (enriched) was obtained by a Fourier transform after acquiring 2000 scans at a spinning speed of 4 kHz. The recycle delay of all experiments utilizing cross polarization was 10 s. A variable MAS speed experiment was conducted with spinning speeds from 0.75 to 4 kHz. Spin-lattice relaxation experiments in the static frame (T_1) and the rotating frame ($T_{1\rho}$) were conducted at room temperature and using delay times of up to 1500 s and 150 ms, respectively. After these experiments were completed, the data required for a useful DD–MAS spectrum was available (T_1 relaxation data) and the MAS–DD spectrum was obtained using a recycle delay of 2600 s and an MAS speed of 4 kHz. A solid-state CP–MAS–DD ^{13}C-NMR spectrum of the enriched **B-a** was acquired utilizing the techniques mentioned above but with a recycle delay of 2 s, a contact time of 800 μs, and 2000 transients.

B-a was cured at two different temperatures: 150 and 200°C. ^{15}N-CP–MAS–DD spectra were obtained at various stages in the polymerization process. A minimum of 2000 transients were accumulated for the curing spectra using the CP–MAS–DD techniques. The number of scans required for sufficient signal to noise (S/N) increased during cure at both temperatures.

RESULTS

Chemical-shift calculations for the structures present in Figure 1(a–c) are shown in Table I. Examples of variable contact time curves are shown in Figure 4 for the observed ^{15}N resonances at 78 and 71 ppm. The cross-polarization parameters, T_{CH} and T_{HH}, are given in Table II. These parameters were comparable for the strong resonances of 71 and 78 ppm, but were notably different for the weaker peaks at 74 and 67 ppm. The CP–MAS–DD spectrum of **B-a** is shown in Figure 5 at full resolution as well as at vertical expansion to show the weaker resonances. The

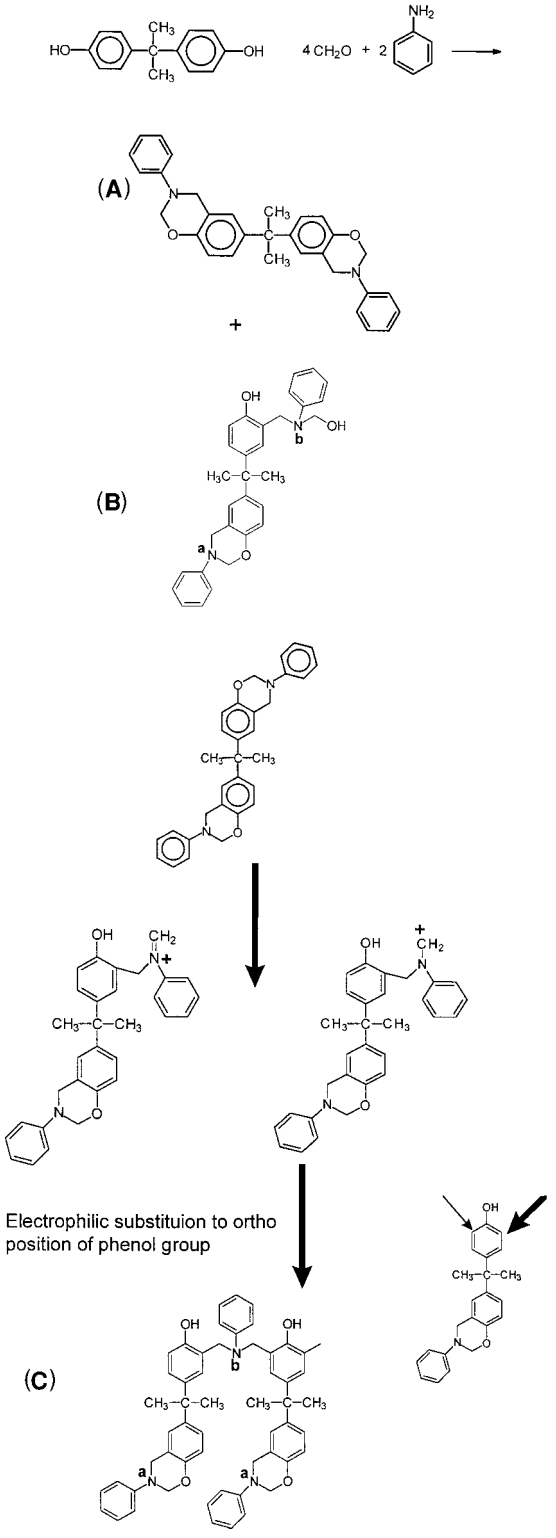

Figure 1 (a) Synthesis of **B-a;** (b) cationic polymerization of **B-a;** (c) side reaction of **B-a.**

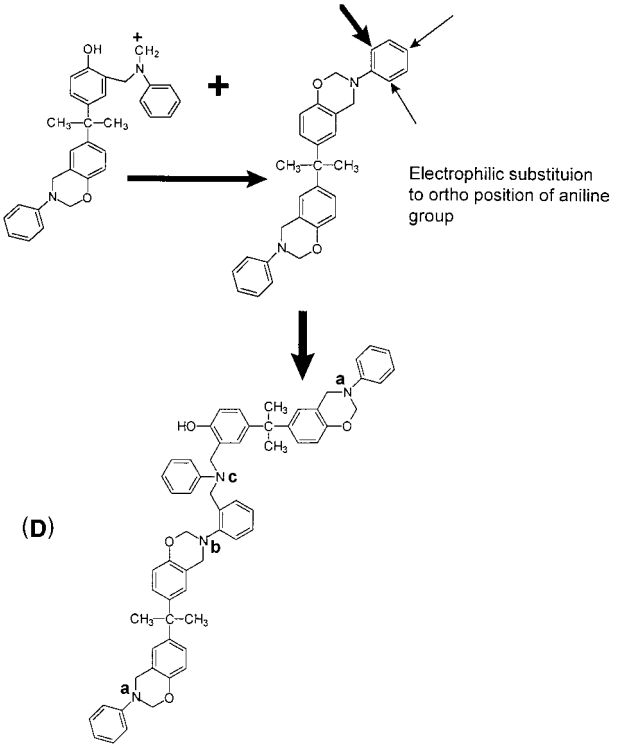

Figure 1. (*Continued*)

CP–MAS–DD and MAS–DD spectra are compared in Figure 6. The spectra of the variable-speed MAS experiment are shown in Figure 7. The corresponding reduction in line width versus spinning speed of the 78 ppm resonance is given in Figure 8 and levels off at approximately 4 kHz. The spin-lattice relaxation curves (for T_1 and $T_{1\rho}$) are shown in Figures 9 and 10, respectively, with the relaxation times given in Table II. The $T_{1\rho}$ relaxation times of the major ^{15}N resonances were similar, while the T_1 relaxation times were considerably different. Figure 11 shows a comparison of the experimental and theoretically calculated chemical shifts.

Some of the ^{15}N-NMR spectra taken during the cure study at 150°C are shown in Figure 12. Changes in peak areas were observed for all peaks at both cure temperatures. The two weaker resonances at 74 and 67 ppm increased initially during cure at both temperatures and then began decreasing approximately 35 min at 200°C and after approximately 2.5 h at 150°C as shown in Figures 13 and 14. The area of the benzoxazine ring resonance (78 ppm) and the polymer backbone resonance (71 ppm) are shown in Figures 15 and 16 for 150 and 200°C, respectively. The benzoxazine ring resonance at 78 ppm decreased during cure at both cure temperatures. However, the peak at 71 ppm (nitrogen bridge structure) initially remained relatively

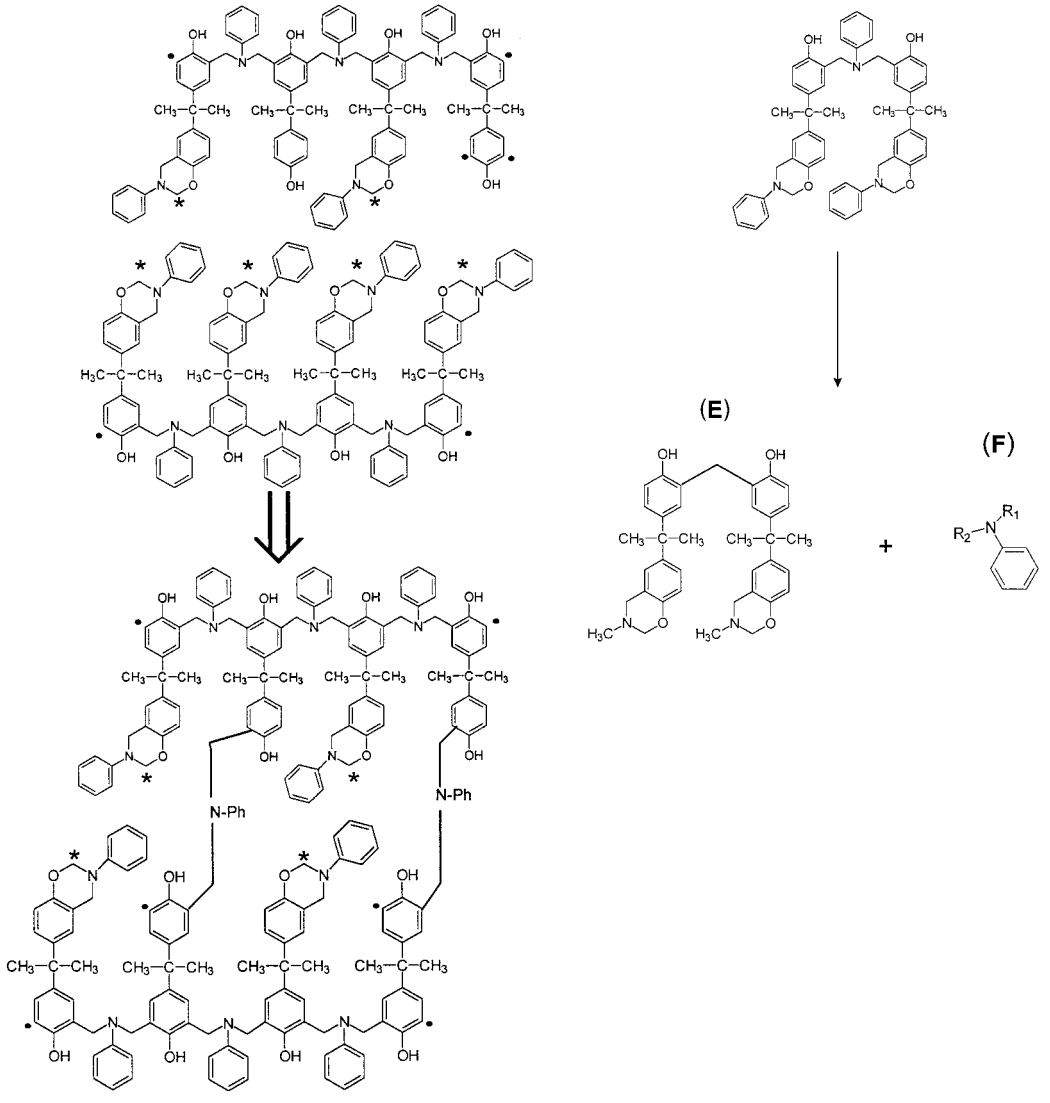

Figure 2 (a) Cross links between two polymer molecules of PBA; (b) degradation of PBA polymer at high temperature.

constant during cure at 200°C and then increased after approximately 40 min.

All resonances broadened significantly during curing at both temperatures. The line width of the 78 and 71 ppm resonances are shown in Figures 17 and 18 for 150 and 200°C, respectively.

DISCUSSION

The calculated chemical shifts for the structures of Figure 1(a–c) are given in Table I. These calculations are based on the chemical structure and use correlations between ^{13}C and ^{15}N resonance positions.[16] However, it has been shown that ^{15}N-NMR chemical shifts are also sensitive to hydrogen-bonding effects in solution.[17,18] Further, it has been shown that there is significant hydrogen bonding in these kinds of benzoxazine compounds.[19] However, in solid-state NMR, it is expected that hydrogen bonding may shift resonances only slightly, but, more importantly, may lead to an increased line width. Referring to Table I, there is good agreement between the observed resonances and the calculated chemical shifts as shown in Figure 11. The 78-ppm peak is assigned to the nitrogen of the unopened benzoxazine ring. It is present in both the monomer structure and that part of the polymer structure containing unopened benzoxazine rings. The resonance at 71

Table I Chemical-shift Calculations for B-a Monomer and Polymer Structures

Compound	Calculation	Value (ppm)	Observed (ppm)
Benzoxazine ring			
Monomer (**A**)	$(27.7 + 17 + 9 + 4) \times 1.36 + 1$	79.4	78
By-product (**B-a**)	"		
Polymer (**C-a**)	"		
Product (**D-a**)	"		
Product (**D-b**)	$(27.7 + 14 + 9 + 4) \times 1.36 + 1$	75.4	74
Mannich bridge Tc			
Polymer (**C-b**)	$(16.3 + 17 + 2\,(10)) \times 1.36 + 1$	72	71
Product (**D-c**)	$(16.3 + 17 + 9 + 7) \times 1.36 + 1$	68.0	67
By-product (**B-b**)	$(16.3 + 17 + 10 + 10) \times 1.36 + 1$	73.5	74

ppm is assigned to the nitrogen bridge structure of the polymer backbone. One other possible product of the **B-a** synthesis reaction is shown in Figure 1 (structure **B**). The observed chemical shift (74 ppm) shows good agreement with the calculated chemical shift of 73.5 ppm for this structure. The normal polymerization pathway is shown in Figure 1(b) and involves the electrophilic substitution between the carbocation and a benzene ring. This transfer has been shown to occur preferentially at free *ortho* and *para* positions of a phenol group.[20] In the case of **B-a,** aromatic sites *ortho* to the phenol oxygen are open and, therefore, this is where electrophilic substitution of the carbocation would occur. This leads to the polymer structure (**C**) which gives the ^{15}N resonance at 71 ppm corresponding to the nitrogen bridge structure.

The presence of the 74, 67, and 71 ppm peaks in the monomer sample indicates that there are dimer and higher oligomers in the as-synthesized sample and possibly product **B** present in the monomer. This is expected since no purification attempts were made due to the limited amount of ^{15}N-enriched sample.[15]

The ^{13}C-CP–MAS–DD spectrum of the enriched **B-a** sample and the natural abundance sample showed good agreement in peak positions. There is also a noticeable increase in the ^{13}C resonance around 97 ppm which was assigned to

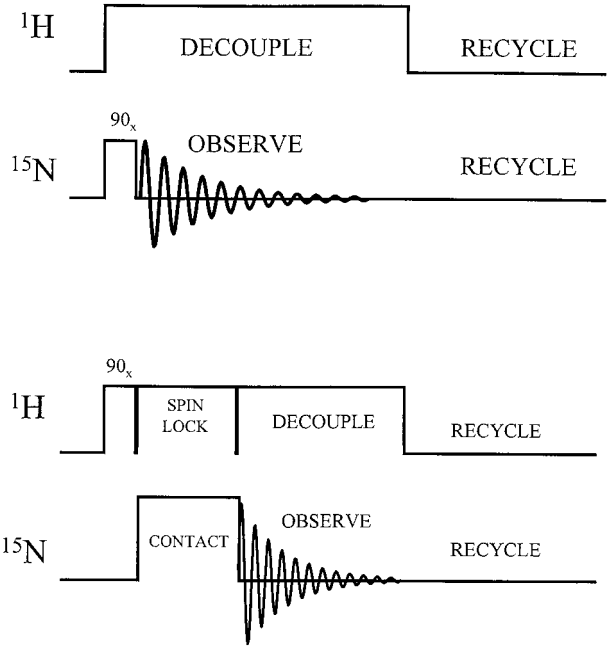

Figure 3 ^{15}N-NMR pulse sequences for HPDEC and CP–MAS.

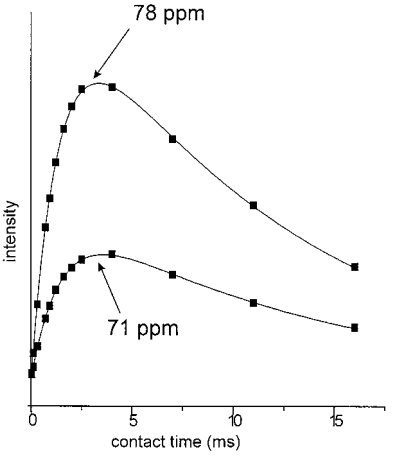

Figure 4 Variable contact cross-polarization curve for strong nitrogen resonances (78 and 71 ppm).

Table II Cross-polarization and Relaxation Data

Peak	T_{CH} (ms)	T_{HH} (ms)	T_1 (s)	$T_{1\rho}$ (ms)
78 ppm	1.4	11.2	700	12
71 ppm	1.5	11.6	490	14
74 ppm	0.94	17		11
67 ppm	0.73	21		17

the CH_2 carbon in the oxazine ring between the oxygen and the nitrogen. This peak could not be confirmed in the previous ^{13}C-NMR study of **B-a** because of its broad line width and low intensity. This peak is more intense in the enriched sample as there are a greater number of ^{15}N—^{13}C structures present (which give rise to sharper resonances) as opposed to the ^{14}N—^{13}C structures of which the quadrupolar ^{14}N broadens the ^{13}C observed resonance. Therefore, the ^{13}C spectrum of enriched **B-a** was useful in completing the ^{13}C spectral assignments of our previous work.[1]

The $T_{1\rho}$ data indicate that the mobility of the 78, 74, and 71 ppm resonances are similar. It has been shown that the spin-lattice relaxation in the rotating frame ($T_{1\rho}$) is sensitive to chain motion.[21,22] These kinds of motion are similar for a nitrogen in the backbone of a polymer as compared to the nitrogen of a side chain on the same polymer molecule. Thus, it is expected that $T_{1\rho}$ would be comparable for the monomer and polymer ^{15}N resonances, which is shown in Table II. The longer $T_{1\rho}$ time for the 67 ppm suggests that the nitrogen source of this resonance is significantly less mobile than are the other structures. The cross-polarization data is consistent with this result since the 67 ppm peak shows a T_{CH} transfer time of 0.73 ms which is much shorter than for the other resonances. T_{CH} is very dependent on the rigidity of a structure and, thus, a short T_{CH} corresponds to a rigid structure surrounding the atom under observation. The structure proposed for the 67 ppm resonance [**D-c** of Fig. 1(c)] may be more rigid than its counterparts due to its configuration and possible addition of other side groups at the *ortho* and *para* positions of the aniline group. The formation of **D** is one that is favored, but no direct evidence for this structure has been given. The electron-donating nature of the nitrogen atom of the aniline group is expected to have a behavior similar to the phenol oxygen in which aromatic sites *ortho* and *para* to the nitrogen atom are made electron-rich. These sites would then be preferred for electrophilic substitution of the carbocation. The data presented here are compatible with

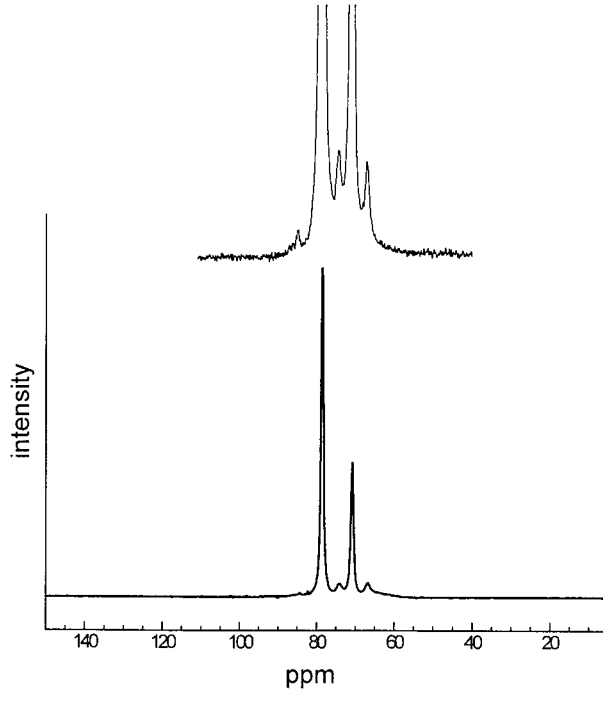

Figure 5 ^{15}N-NMR spectrum of PBA monomer.

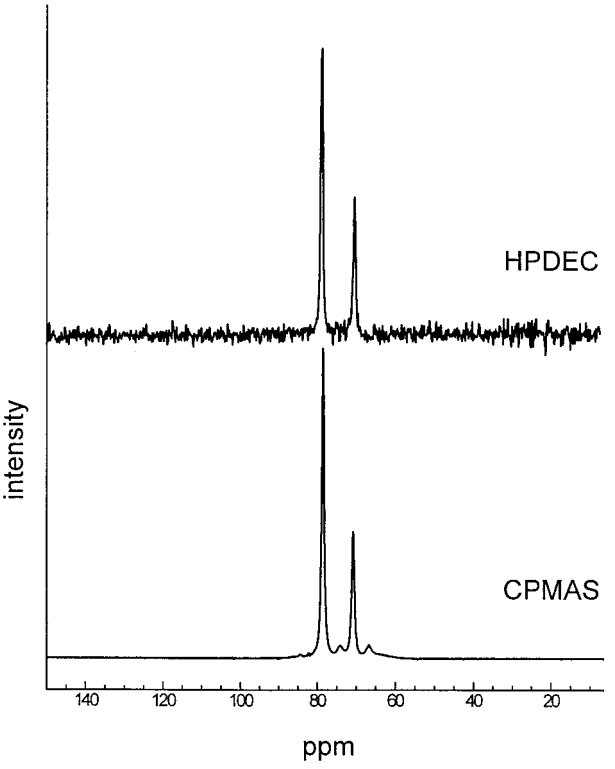

Figure 6 ^{15}N-CP-MAS and HPDEC spectra of PBA.

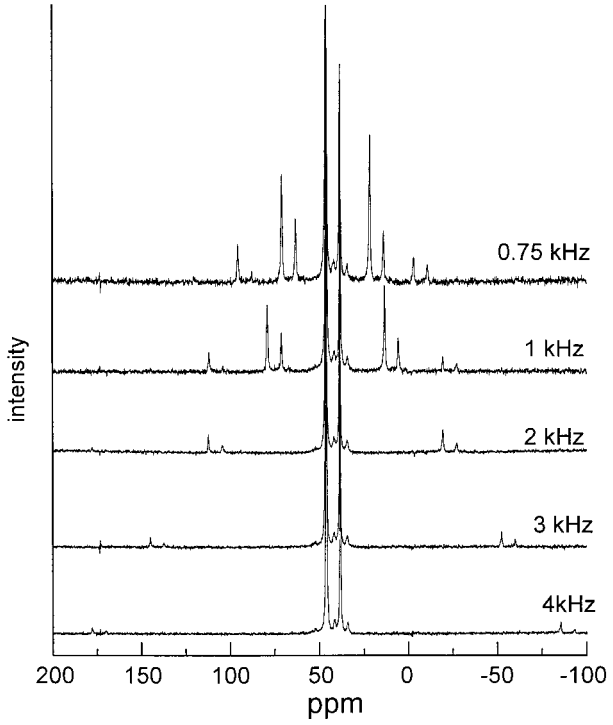

Figure 7 ^{15}N-CP-MAS spectra of PBA at spinning speeds from 0.75 to 4 kHz.

the existence of the structures formed by such a reaction [structure **D** of Fig. 1(c)].

In regard to the peak at 71 ppm, the spin-lattice relaxation time (T_1 = 490 s) is significantly shorter than the T_1 of the benzoxazine ring peak at 78 ppm (T_1 = 700 s). Since T_1 is sensitive to localized motion, it is expected that the

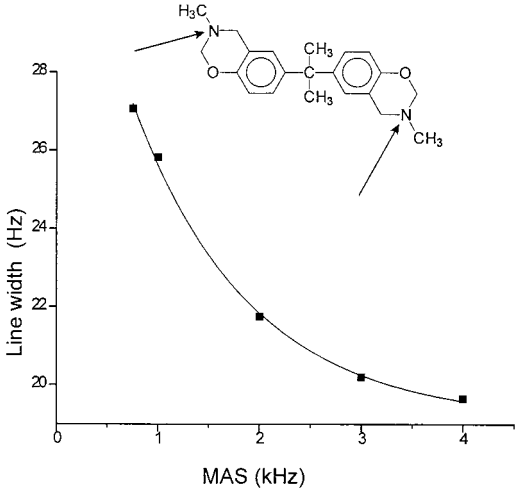

Figure 8 Line width versus MAS speed for 78-ppm nitrogen resonance.

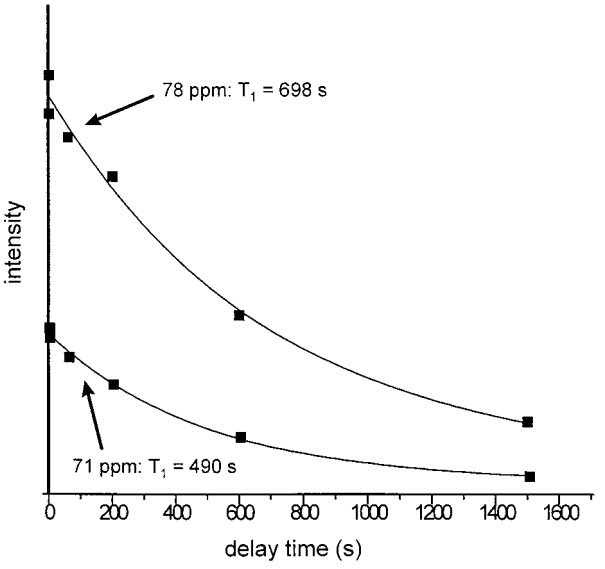

Figure 9 ^{15}N spin-lattice relaxation (T_1) decays for 78 and 71 ppm resonances.

restricted motion of a ring structure would result in a longer T_1 in the benzoxazine ring. After the T_1 data were available, the MAS–DD spectrum of **B-a** was acquired and compared to the CP–MAS–DD spectrum (Fig. 6). These spectra are comparable in the main observed resonances, but the signal to noise (S/N) of the MAS–DD spectrum is much poorer. Further, the MAS–DD spectrum took approximately three times the time to acquire as compared to the CP–MAS–DD spectrum. This illustrates the importance of using cross po-

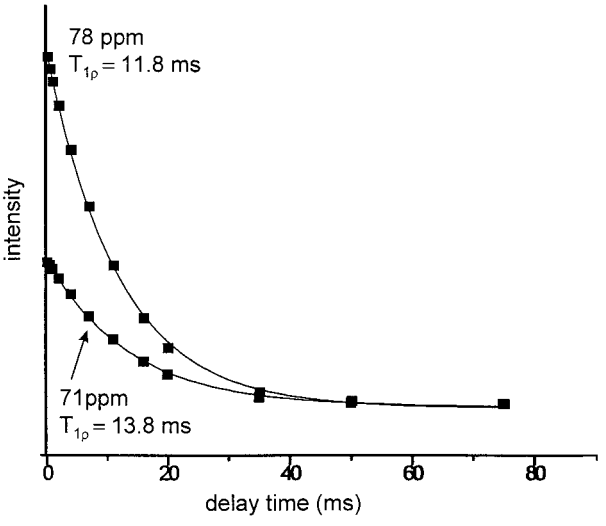

Figure 10 ^{15}N spin-lattice relaxation in the rotating frame ($T_{1\rho}$) decays for 78 and 71 ppm resonances.

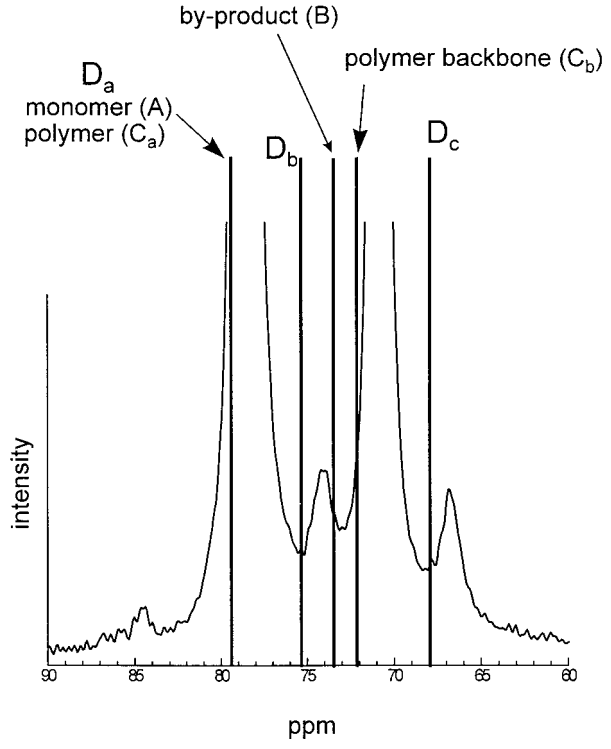

Figure 11 Calculated ^{15}N chemical shifts compared to observed spectrum of PBA.

larization in this study. Not only is there a large improvement in the S/N ratio, but experiments may be run in much less time when cross polarization is utilized.

The benzoxazine ring peak of 78 ppm decreased during cure at both temperatures as shown in Figures 15 and 16. Since the breaking of the benzoxazine ring is one of the main processes occurring during polymerization, this is the expected result. However, the resonances due to the intermediate structures (74 and 67 ppm) behaved differently. Initially, these peaks increased with cure time. However, an inflection point was observed at approximately 35 min total cure time at 200°C (Fig. 14), after which time the resonance decreased in area and was unobservable after 1-h cure time. The cure study at 150°C showed similar results. The intermediate peaks of 74 and 67 ppm increased initially and reached an inflection point at approximately 2.5 h (Fig. 13).

The reaction rate for **B-a** was shown by differential scanning calorimetry (DSC) to have a maximum at about 10 min at 200°C and about 70 min at 160°C.[23] The maximum concentration of the intermediates in the present work occurs at about 35 min at 200°C and about 2.5 h at 150°C. Considering the fact that the sample holder used in these curing experiments is made of zirconia, which is a thermal insulator, and the fact that curing was done in increments where some time was spent warming the sample up to the actual curing temperature, it is expected that the results presented here show a delay compared to the DSC results. Further, the 3-h peak intensity of the intermediates at 150°C is expected to be longer than the 160°C reaction rate maximum as shown by the DSC because of the decrease in temperature. A decrease in temperature between 170 and 160°C led to an increase in the time of maximum reaction rate of about 1.5-fold.[23] Therefore, the 2.5-h maximum in the intermediates is not unexpected.

The degradation reaction shown in Figure 2(b) could not be confirmed by the data presented in this work. However, the occurrence of this reaction would coincide with a decay in the S/N which was observed for both cure temperatures. The

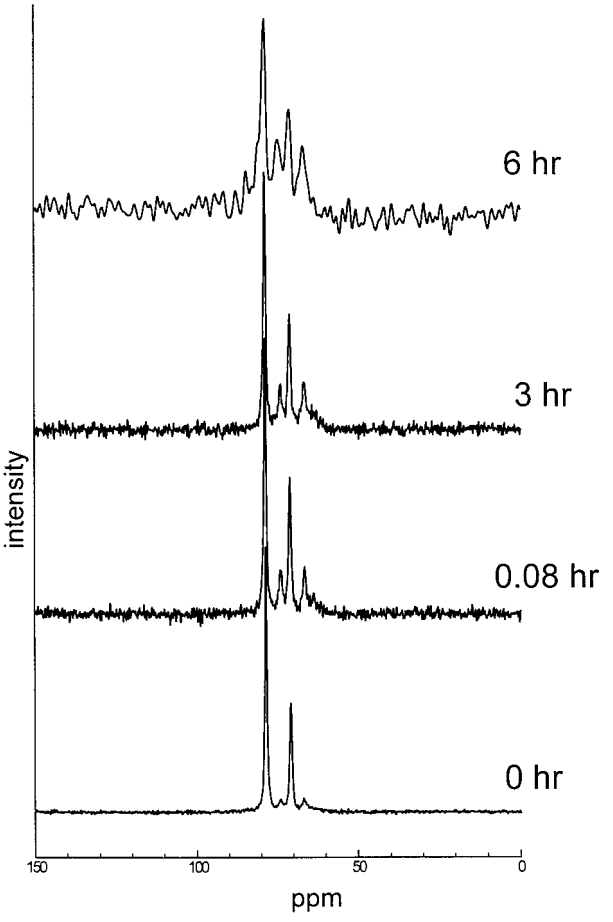

Figure 12 ^{15}N-NMR spectra taken during cure at 150°C.

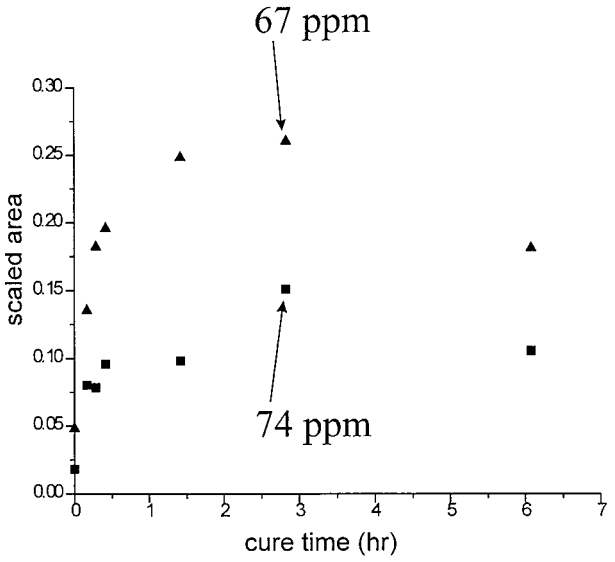

Figure 13 Change in area of 74 and 67 ppm peaks at 150°C.

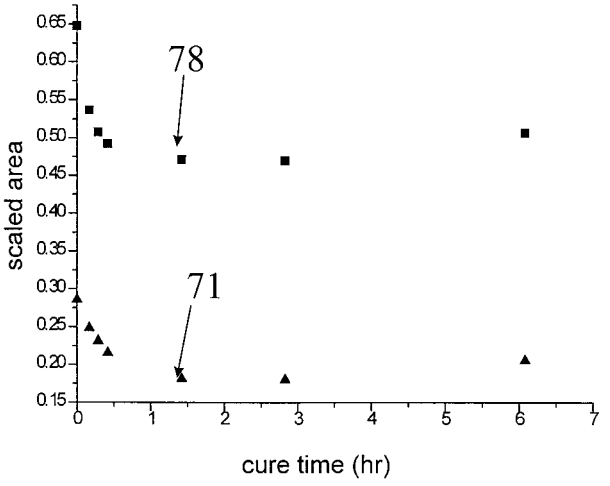

Figure 15 Change in area of 78 ppm (polymer) and 71 ppm (benzoxazine ring) peaks at 150°C.

formation of structures **E** and **F** of Figure 2(b) would not be directly detectable because structure **E** has no nitrogen atoms and structure **F** would be given off as a gas at the cure temperatures used. The observed decrease in the S/N ratio would also be expected due to the polymerization and crosslinking of the polymer.

All the observed peaks exhibited line-width broadenings at both cure temperatures. The

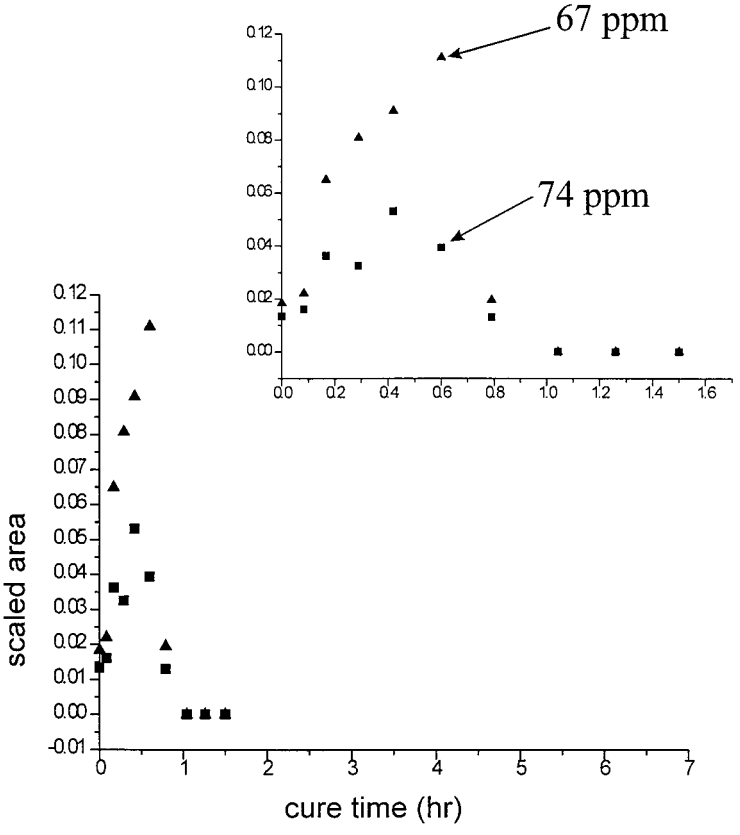

Figure 14 Change in area of 74 and 67 ppm peaks at 200°C.

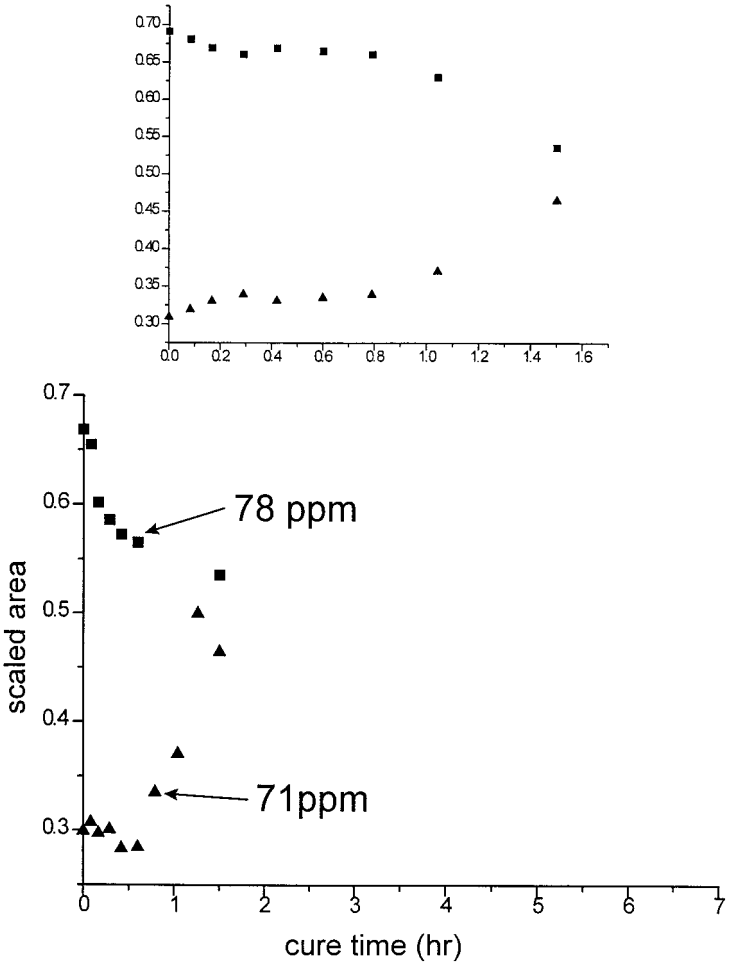

Figure 16 Change in area of 78 ppm (polymer) and 71 ppm (benzoxazine ring) peaks at 200°C.

change in line width for the 78 and 71 ppm resonances are shown in Figures 18 and 19 for 200 and 150°C, respectively. The nature of the NMR line width is dependent on several factors: The first factor is the homogeneity of the main magnetic field (B_0). If the magnetic field remains uniform over the time in which an NMR study is performed, then this remains constant for each cure interval. The NMR line width is also dependent on spin–spin relaxation (T_2) as well as chemical-shift anisotropy (CSA). The T_2 of an atom is dependent on the motions of the molecule and, hence, is one indicator of the mobility of a molecular segment. The CSA is a measure of the variability of similar chemical structures. For a monodisperse polymer, CSA would be very low and would increase with polydispersity. It has been shown for polymer systems that the line width increase of a cured polymer system is due

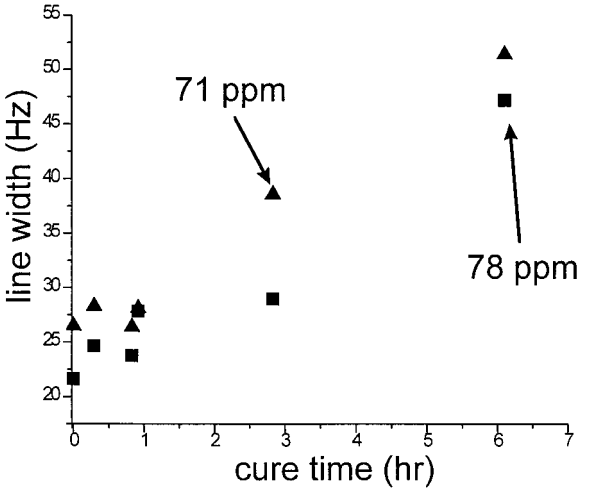

Figure 17 Line width versus cure time at 150°C for 78 and 71 ppm resonances.

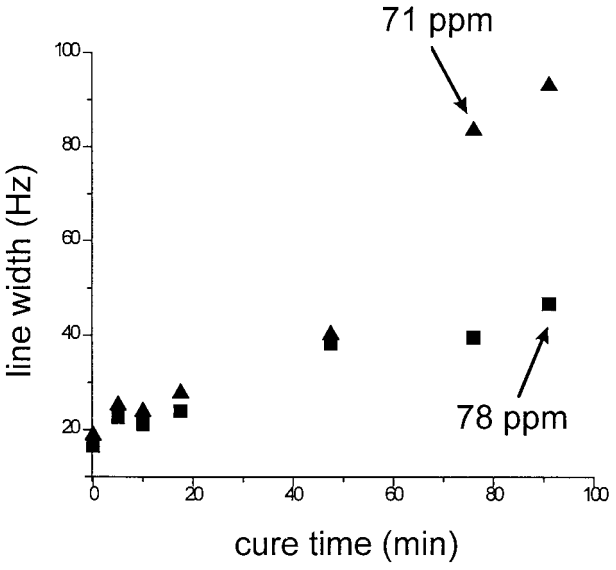

Figure 18 Line width versus cure time at 200°C for 78 and 71 ppm resonances.

mainly to chemical-shift anisotropy and not to T_2.[24] For the current work, the line widths change substantially, as was observed in an earlier ^{13}C-NMR cure study of the same compound.[1] It will be assumed that the major contributing factor to the increase in line width is chemical-shift anisotropy. However, from the current data, it is not possible to determine how much of the line broadening is due to polymerization and how much is due to crosslinking. As mentioned earlier, hydrogen bonding may also be responsible for line broadening, but this effect is not expected to increase substantially during polymerization.

CONCLUSION

An ^{15}N-enriched sample of a 3,4-dihydro-3-substituted-1,3-benzoxazine, **B-a,** was synthesized and characterized using ^{15}N solid-state NMR spectroscopy. The observed resonances agreed well with the calculated chemical shifts of the monomer, polymer, and alternate product structures. The cross-polarization and relaxation analysis supported the assignments made from the chemical-shift data. The cure studies showed intensity changes and line-width broadenings which are attributed to the polymerization as well as to the cross linking of the compound. These results showed that the polymerization progressed at a much higher rate at 200°C as opposed to 150°C.

REFERENCES

1. V. M. Russell, Ph.D. thesis, *Case Western Reserve University, Cleveland, OH,* 1996.
2. R. L. Bryson, G. R. Hatfield, T. A. Early, A. R. Palmer, and G. E. I. Macie, *Macromolecules,* **16,** 1669 (1983).
3. P. Sohar, G. Bernath, S. Frimpong-Manso, A. E. Szabo, and G. Stajer, *Magn. Reson. Chem.,* **28,** 1045 (1990).
4. K. Neuvonen and K. Pihlaja, *Magn. Reson. Chem.,* **28,** 239 (1990).
5. K. V. Prasad Rao, P. S. N. Reddy, and V. Sundaramurthy, *Magn. Reson. Chem.,* **24,** 644 (1986).
6. K. Neuvonen, R. Pohtola, and K. Pihalja, *Magn. Reson. Chem.,* **27,** 725 (1989).
7. K. Neuvonen and K. Pihlaja, *ACTA Chem. Scand.,* **47,** 695 (1993).
8. G. R. Hatfield and G. E. Maciel, *Macromolecules,* **20,** 608 (1987).
9. W. G. Proctor and F. C. Yu, *Phys. Rev.,* **77,** 716 (1950).
10. J. Schaefer, E. O. Stejskal, S. Gacob Gary, and R. A. McKay, *Appl. Spectrosc.,* **36,** 179 (1982).
11. H. R. Kricheldorf, *Pure Appl. Chem.,* **54,** 467 (1982).
12. M. Andreis and J. L. Koenig, *Adv. Polym. Sci.,* **124,** 191 (1995).
13. C. L. Levy and R. L. Lichter, *Nitrogen-15 Nuclear Magnetic Resonance Spectroscopy,* Wiley, New York, 1979.
14. W. Witanowski, L. Stefaniak, and G. A. Webb, *Annu. Rep. NMR Spectrosc.,* **18,** 1 (1986).
15. X. Ning and H. Ishida, *J. Polym. Sci. Part B Polym. Phys.,* **32,** 921 (1994).
16. R. O. Duthaler and J. D. Roberts, *J. Am. Chem. Soc.,* **100,** 3889 (1978).
17. B. L. Gaffney, P. P. Kung, C. Wang, and R. A. Jones, *J. Am. Chem. Soc.,* **117,** 12281 (1995).
18. M. Witanowski, W. Sicinska, Z. Grabowski, and G. A. Webb, *J. Magn. Reson. A,* **104,** 310 (1993).
19. H. Ishida and C. M. Krus, *Macromolecules,* to appear.
20. G. Riess, J. M. Schwob, G. Guth, M. Roche, and B. Lande, in *Advances in Polymer Synthesis,* B. M. Culbertson and J. E. McGrath, Eds., Plenum, New York, 1985.
21. J. Schaefer, E. O. Stejskal, and R. Buchdahl, *Macromolecules,* **10,** 384 (1977).
22. J. R. Pratt and T. L. St. Clair, *SAMPE J.,* **26,** 29 (1990).
23. H. Ishida and Y. Rodriguez, *Polymer,* **36,** 3151 (1995).
24. A. D. Bain, D. R. Eaton, A. E. Hamielec, M. Mlekuz, and B. G. Sayer, *Macromolecules,* **22,** 3561 (1989).